When Weak Inhibition Synchronizes Strongly Desynchronizing Networks of Bursting Neurons

Igor Belykh and Andrey Shilnikov

Department of Mathematics and Statistics and The Neuroscience Institute, Georgia State University, 30 Pryor Street, Atlanta, Georgia 30303, USA

(Received 6 January 2008; published 13 August 2008)

We show that weak common inhibition applied to a network of bursting neurons with strong desynchronizing connections can induce burst and complete synchronization. We demonstrate that the weak synchronizing inhibition from the same pacemaker neuron can win out over much stronger desynchronizing connections within the network, provided that the neuron's duty cycle is sufficiently long. We also gain insight into how the changes in burst duty cycles can trigger unexpected clusters of synchrony in bursting networks.

DOI: 10.1103/PhysRevLett.101.078102 PACS numbers: 87.19.lm, 05.45.Xt, 87.19.lj

Neurons can generate a complex oscillatory rhythm known as bursting, consisting of a rapid sequence of spikes followed by a quiescent state. There has been much work on mechanisms that generate such bursting [1–4]. Interacting bursting neurons may exhibit different forms of synchrony, including synchronization of individual spikes, burst synchronization when only the envelopes of the spikes become synchronized, and complete synchrony [5,6]. The emergence of the synchronous rhythms in a neuronal network is closely related to the properties of the individual bursting neurons, a type of synaptic coupling, and network topology [5–12]. In particular, inhibitory connections, slow or fast, have been shown to play multiple roles in promoting synchrony or fostering asynchronous activities in bursting networks [7–11]. More precisely, it has been found that a slow decay of inhibition, or a time-delay, is needed to established a synchrony in the network [8]. The underlying architecture of an inhibitory network also plays an important role in synchronizing or desynchronizing the network. For example, synchronization in an inhibitory network of two bursting neurons, interconnected via fast nondelayed synapses is typically unstable. Here, the desynchronizing inhibition can lead to asynchronous or antisynchronous behavior [7]. This carries over to larger interconnected inhibitory networks [10]. At the same time, a common fast inhibition of a neuronal network received from one or several pacemaker neurons was shown to favor synchronization [11]. It was also shown in [11] that a small amount of electrical coupling, added to already significant common inhibition of the network can increase the synchronization more than a very large increase in the synchronizing inhibitory coupling. Central pattern generators (CPGs) and other neural circuits are often composed of pairs of mutually inhibiting cells, driven by a common bursting pacemaker [13,14]. Understanding the emergence of different antiphase and synchronous rhythms in such networks requires an in-depth knowledge of the interplay among mutual internal inhibition, common external driving, and temporal characteristics of neurons composing the network.

In this Letter, we report our counterintuitive result that weak common inhibition applied to a network of neurons with strong desynchronizing connections can induce its synchronization. More precisely, we consider an inhibitory network of bursting neurons that are all driven by the same pacemaker neuron(s). The desynchronizing inhibitory coupling within the network is much (e.g., a hundred times) stronger than the common, external inhibition. We show that the weak synchronizing inhibition can overcome the contribution of the strongly desynchronizing coupling, provided that the pacemaker's duty cycle, the fraction of the period during which the neuron bursts, is sufficiently long. We reveal the general mechanism of induced synchronization and show how neurons' duty cycles are used to induce clusters of synchrony in larger inhibitory networks of bursting neurons.

We consider a heterogeneous network of bursting interneurons [3] with fast inhibitory connections modeled, within the Hodgkin-Huxley framework, by the following equations:

$$\begin{aligned} CV_i' &= F(V_i, h_i, m_i) - (V_i - E_s)\sum_{j=1}^{n} g_{ij}\Gamma(V_j - \Theta_{\mathrm{syn}}), \\ h_i' &= [f(500, 0.0325, V_i) - h_i]/\tau_{\mathrm{Na}}, \\ m_i' &= [f(-83, 0.018 + V_i^{\mathrm{shift}}, V_i) - m_i]/\tau_{\mathrm{K2}}, \; i, j = \overline{1, n}, \end{aligned} \tag{1}$$

where $F(V_i, h_i, m_i) = -[30m_i^2(V_i + 0.07) + 8(V_i + 0.046) + 160h_i(V_i - 0.045)\{f(-150, 0.0305, V_i)\}^3 + 0.006]$ and $f(a, b, V_i) = 1/(1 + e^{a(V_i+b)})$. Here, the ith neuron variables V_i, h_i, and m_i are the membrane potential, opening probabilities of the sodium and potassium channels, respectively. Because of the disparity of the time constants $\tau_{\mathrm{Na}} = 0.0405$ and $\tau_{\mathrm{K2}} = 0.9$, the system (1) possesses two characteristic time scales: the voltage and the sodium current are the fast variables, while the potassium current is a slow one. It is known that the dynamics of the individual slow-fast system composing the network is centered around stable manifolds formed by the limit sets of the fast

subsystem. The model possesses two such manifolds constituting a skeleton of bursting activity: 2D spiking and 1D quiescent, M_{eq}, manifolds, composed of limit cycles and equilibria of the fast system. The individual model exhibits square-wave bursting; the bursting solution traverses along and repeatedly jumps between these manifolds (see Fig. 1). In it, the solid blue S-shape curve M_{eq} and the dark yellow surface $m' = 0$ are two nullclines of the fast and slow systems, respectively. They are often called fast and slow nullclines. By construction, a point of intersection of M_{eq} with the slow nullcline, $m' = 0$, is an equilibrium state of the corresponding neuron. Further details on the dynamics of uncoupled equations (1) can be found in [3]. Here, V_i^{shift} is the intrinsic, bifurcation parameter governing the temporal characteristics of bursting cells. In network (1), the synapses are fast and nondelayed [6]. The reversal potential $E_s = -0.0625$ is set to make all synapses inhibitory. The parameter g_{ij} is the strength of the synaptic coupling from neuron i to neuron j. The synaptic coupling is modeled using the sigmoidal function [10], $\Gamma(V_j - \Theta_{\text{syn}}) = 1/[1 + \exp\{-1000(V_j - \Theta_{\text{syn}})\}]$, where $\Theta_{\text{syn}} = -0.03$ is the synaptic threshold.

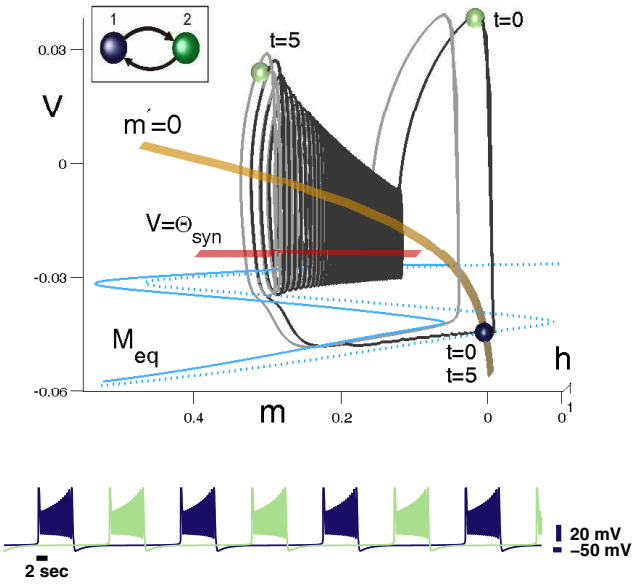

FIG. 1 (color online). Half-center oscillator composed of inhibitory neurons (1). The neurons are identical ($V_{1,2}^{\text{shift}} = -0.02$); the inhibitory connections are strong ($g_{12} = g_{21} \equiv g_S = 2$). (Top) The uncoupled and inhibited nullclines are depicted by solid and dotted blue lines, respectively. Color-matching balls represent the instant phase points of the cells on the bursting orbit. The dark gray trajectory corresponds to the antiphase solution, while the light one is the reference trajectory of the uncoupled cell. As soon as the active (green) cell is above the threshold Θ_{syn}, the nulcline M_{eq} is shifted towards the slow nullcline $m' = 0$ to generate a stable equilibrium state near the lower knee through the saddle-node bifurcation. The inactive (blue) cell is trapped at it until the active cell falls down to M_{eq}. (Bottom) Time series of the established antiphase dynamics. Note the delayed postinhibition firing of the inactive cell due to the slow passage throughout the vicinity of the disappeared saddle node.

I. Half-center oscillator.—Consider first a pair of bursting neurons (1) with reciprocally inhibitory couplings. This network, called a half-center oscillator, is a principal building block of various CPGs [13] that produces antiphase oscillations [10]. By geometry of the nullclines, each uncoupled cell has a single, unstable equilibrium state located away from the stable, hyperpolarized branch of M_{eq}. The effect of inhibition from one cell to the other is to shift the S-shape nullcline M_{eq} towards the slow nullcline $m' = 0$ in the phase space of the inhibited cell. If inhibition is sufficient, this creates a new stable equilibrium around the lower knee of M_{eq} through a saddle-node bifurcation (Fig. 1). We will refer to this stable equilibrium state as a lock-down state. Cutting inhibition off makes this equilibrium state disappear through the reverse saddle-node bifurcation. This bifurcation has a remarkable feature of the bifurcation memory, revealed through a specific, scalable delay of the flight time of the phase point passing throughout a vicinity of the disappeared saddle-node. While spiking, the active cell keeps oscillating around the synaptic threshold Θ_{syn}, rapidly switching inhibition of the inactive cell on and off. Therefore, the inhibiting current emerges periodically for a period shorter than the characteristic escape time of the inactive cell. Hence, the latter is trapped and oscillates around the lower knee of the inhibited nullcline, depicted by the dotted blue line in Fig. 1. The active cell eventually reaches the end of the spiking manifold and falls down to M_{eq}. This changes the governing nullcline for the other cell and releases it from inhibition. Therefore, the released cell jumps up and turns inhibition of the other cell on. This process of switching between active and inactive states of the two cells is cyclic and results in the onset of antiphase bursting. A similar hold-then-release mechanism of the antiphase behavior of spiking cells is often referred to as "synaptic release" [7,10], causing postinhibitory rebound [15]. Below we show that the synaptic release mechanism along with a long duty cycle of driving neurons play the crucial role in inducing synchronization in larger networks.

II. Weak vs strong network.—Inspired by the circuitry of a heart leech CPG [13] and a tritonia CPG governing locomotion [14], we consider their principal subnetwork shown in the left inset of Fig. 2. In this network, codenamed "weak vs strong," neurons 1 and 2 form a half-center pair, receiving common inhibition from neuron 3. The reciprocal inhibition within the pair is strong, and the pair bursts in antiphase in the absence of inhibition from neuron 3. Neuron 3 is assumed to have much weaker unidirectional connections with the pair. In what follows, neuron 3 shall attempt to make the half-center pair burst synchronously, fighting against a much stronger desynchronizing force within the half-center network. It is worth noticing that the weak vs strong ratio of the couplings is

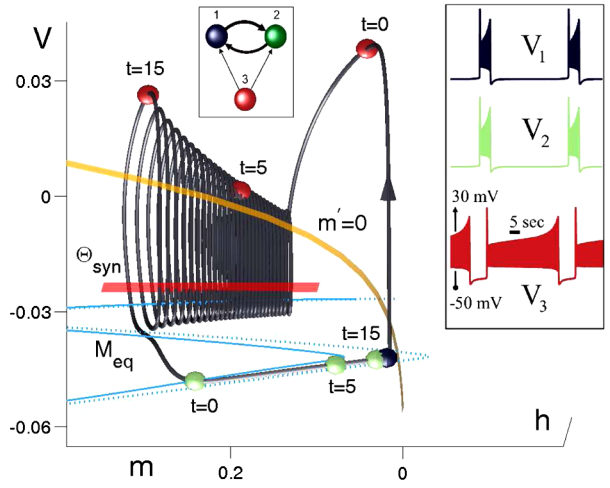

FIG. 2 (color online). Dynamics of the weak vs strong network (left inset) with weak $g_{31} = g_{32} \equiv g_w = 0.02$ and strong coupling $g_S = 2$ for a long duty cycle. The control parameters are $V_{1,2}^{\text{shift}} = -0.02$ and $V_3^{\text{shift}} = -0.024$. Longer burst duration of the driving neuron allows the driven neurons 1 and 2 to get together at the lock-down state near the lower knee of the inhibited nullcline M_{eq}. Neuron 1 (blue ball) is locked by the driving neuron 3, while the phase point of neuron 2 (green ball) moves along M_{eq} towards its lower knee and eventually catches up with the phase state of neuron 1. Having become inactive, the driving neuron 3 releases neurons 1 and 2 from inhibition simultaneously. Jumping up to the spiking manifold, they achieve complete synchronization, shown by the time-series of the established regimes. Note that, when synchronized, neurons 1 and 2 shorten their natural duty cycle.

particularly pronounced in the tritonia CPG [14]. Let us consider two distinct outcomes of this weak vs strong struggle, depending on the duty cycle of the driving neuron 3. To better isolate the key effect, we will only change the duty cycle of the driving neuron 3 while keeping the duty cycle of the neurons forming the half-center constant around 50%.

We set the driving neuron relatively close to the transition from bursting into tonic spiking which is due to either the blue sky bifurcation [3] or the bistability scenario [4]. In either case, the duty cycle grows fast as V_3^{shift} approaches the transition value [3]. This allows the driving neuron 3 to maintain long burst durations without changing the interburst interval. In other words, it spends more time on the spiking manifold than on the lower branch of the nullcline M_{eq}. We start with the duty cycle of 80% which lies in a biologically plausible interval [13]. Recall that due to the antiphase dynamics, either cell of the half-center pair is always inactive, being locked down near the lower knee of M_{eq}. While the phase state of the driving neuron 3 is on the spiking manifold and above the threshold, it also inhibits the inactive cell of the half-center pair, extending its lock-down state further. Note that in the 3D phase space of each individual system, the gap between the S-shape nullcline M_{eq} and the slow nullcline $m' = 0$ is initially small so that a weak inhibition coming from the driving neuron 3 is sufficient to close it and hence to lock the inactive neuron of the half-center pair down. This small gap between the fast and slow nullclines is not a peculiarity of the neuron model (1), but is typical for many other Hodgkin-Huxley-type models, including Sherman and a modified Morris-Lecar ones [2]. Figure 2 shows that the duty cycle of the driving neuron 3 is long enough to put both neurons 1 and 2 into the lock-down state and therefore synchronize them. For the given synaptic threshold Θ_{syn}, this results in complete synchronization. It is important to emphasize that weak common inhibition is unable to establish burst or complete synchronization within the half-center network if the duty cycle of the driving neuron 3 is short, typically shorter than 50% In this case, neuron 2 does not have enough time to catch up with neuron 1. Released from inhibition, neuron 1 is free to fire a first action potential in a burst, while neuron 2 remains yet inactive. After jumping up, the phase point of neuron 1 crosses the synaptic threshold and turns the strong inhibition within the half-center network on. It makes neuron 2 locked down until neuron 1 is out of its active phase. This leads to the antiphase behavior of the half-center pair, described in Fig. 1. Thus, an effort of the driving neuron 3 to break down the antiphase firing rhythm of the half-center pair fails. Figure 3 shows that the driving neuron 3 with a duty cycle shorter than about 50% cannot synchronize the given half-center pair, even if the strength of common inhibition exceeds that of reciprocal inhibition within the half-center network. It clearly reveals *two* key components of the mechanism, underlying the onset of induced synchronization in the half-center network. These are (i) the hold-then-release synaptic property, allowing the driving neuron to lock down the half-center oscillator, and (ii) a long duty cycle of the driving neuron. Consequently, the synchronization mechanism is not restricted to square-wave bursting, but is applicable to other types of bursters, allowing for the synaptic release mechanism and therefore, forming a half-center oscillator. Figure 3 shows a wide horizontal plateau in the duty cycle-dependence curve of the synchronization threshold coupling. This confirms that the strength of common inhibition, that would be expected to be a third important component, plays no essential role in inducing synchronization, provided that it is sufficient to close the

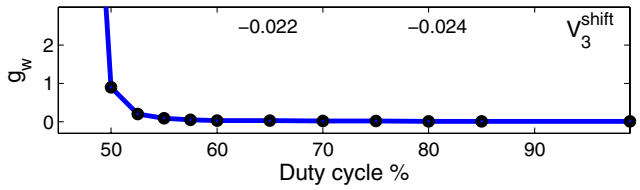

FIG. 3 (color online). Dependence of the threshold coupling strength g_w, inducing synchronization in the half-center network, on the duty cycle of the driving neuron 3. Other parameters are the same as in Fig. 2. Values of V_3^{shift} correspond to the indicated duty cycles.

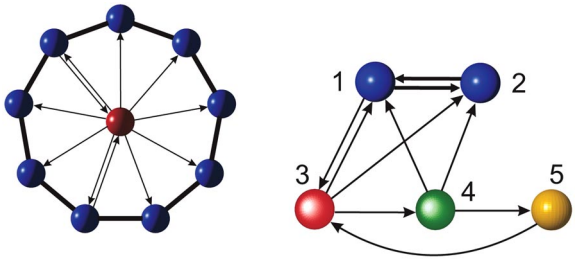

FIG. 4 (color online). Examples of the networks satisfying the assumed synchronization conditions. The neurons of same color form a cluster. The width of the links may be thought of as the coupling strength. Note strong uniform couplings within the cluster and weak connections from the driving neuron/neurons. (Left) Ring network driven by the central pacemaker. Reciprocal inhibitory connections, $g_r = 1$, among neurons within the ring are depicted by links without arrows. Directional connections from the central pacemaker cell to the ring are uniform and weak, $g_d = 0.02$. Two backward connections, $g_b = 0.02$, from the ring are introduced to make the network asymmetric. (Right) Network with an irregular structure. The coupling strengths are set as follows: $g_{12} = g_{21} = 2$, all other $g_{ij} = 0.02$. Note that in contrast with the network of Fig. 2, the input to cells 1 and 2 comes from more than one driving cell. Moreover, the driving cells 3 and 4 are always desynchronized due to the network topology. For $V_i^{\text{shift}} = -0.02$, $i = 1, \ldots, 7$, corresponding to the 50% duty cycle of all the neurons, no synchronization within the clusters of both networks is induced. The longer 80% duty cycle of the driving neuron/neurons arising at $V_{\text{center}}^{\text{shift}} = -0.024$ (left network) and $V_{3,4}^{\text{shift}} = -0.024$ (right network) puts the neurons within the clusters in synchronization.

gap between the nullclines. The induced burst synchronization persists even when the driven neurons are mismatched due to both intrinsic properties of the cells and asymmetries of the network. In particular, it persists even under a 200% mismatch between coupling strengths, like $g_{12} = 1$ and $g_{21} = 3$. Moreover, the inhibitory connections from neuron 3 *do not have* to be unidirectional; for example, symmetric synaptic couplings $g_{13} = g_{31} = 0.02$ and $g_{23} = g_{32} = 0.02$ also induce synchronization in the half-center network.

III. Larger networks.—Our results carry over to larger networks of bursting neurons (1), where subnetworks (clusters) of neurons with strong desynchronizing connections receive a common input from the same driving neurons. Examples of networks with the above properties are depicted in Fig. 4.

In summary, the duty cycle of neurons driving an inhibitory network is shown to be the critical characteristic, explicitly determining synchronization properties of the network. We have shown that a bursting network with strong desynchronizing connections can be synchronized by a weak common inhibitory input from an external pacemaker neuron whose duty cycle is sufficiently long. In strongly heterogeneous networks, the ratio of the duty cycles becomes the imperative order parameter that controls the dynamics of the network and designates its pacemaker by the intrinsic properties, or by the network structure. Thus, the pacemaker being the longest bursting cell makes other strongly uncorrelated neurons synchronized and determines the network's paces and rhythms. The discovered mechanism of induced synchronization is generic and applicable to other Hodgkin-Huxley-type neurons, capable of forming a half-center oscillator. It demonstrates how neurons with different duty cycles can be employed as building elements for constructing complex neuronal networks with prescribed cooperative behaviors.

This work was supported by the GSU Brains and Behavior program, Landau Network-Centro Volta, and RFFI No 050100558.

[1] J. Rinzel, *Lecture Notes in Biomathematics* (Springer-Verlag, Berlin, 1987), Vol. 71, p. 251; D. Terman, SIAM J. Appl. Math. **51**, 1418 (1991); V. N Belykh, I. V Belykh, M. Colding-Joergensen, and E. Mosekilde, Eur. Phys. J. E **3**, 205 (2000); P. Channell, G. Cymbalyuk, and A. Shilnikov, Phys. Rev. Lett. **98**, 134101 (2007).
[2] E. M. Izhikevich, Int. J. Bifurcation Chaos Appl. Sci. Eng. **10**, 1171 (2000).
[3] A. Shilnikov and G. Cymbalyuk, Phys. Rev. Lett. **94**, 048101 (2005).
[4] A. Shilnikov, R. Calabrese, and G. Cymbalyuk, Phys. Rev. E **71**, 056214 (2005).
[5] E. M. Izhikevich, SIAM Rev. **43**, 315 (2001); C. van Vreeswijk and D. Hansel, Neural Comput. **13**, 959 (2001); M. Dhamala, V. K. Jirsa, and M. Ding, Phys. Rev. Lett. **92**, 028101 (2004).
[6] I. Belykh, E. de Lange, M. Hasler, Phys. Rev. Lett. **94**, 188101 (2005).
[7] X.-J. Wang and J. Rinzel, Neural Comput. **4**, 84 (1992).
[8] D. Golomb and J. Rinzel, Phys. Rev. E **48**, 4810 (1993); D. Terman, N. Kopell, and A. Bose, Physica (Amsterdam) **117D**, 241 (1998);R. C. Elson, A. I. Selverston, H. D. I. Abarbanel, and M. I. Rabinovich, J. Neurophysiol. **88**, 1166 (2002); J. Rubin and D. Terman, SIAM J. Appl. Dyn. Syst. **1**, 146 (2002).
[9] T. Lewis and J. Rinzel, J. Comput. Neurosci. **14**, 283 (2003).
[10] N. Kopell and G. B. Ermentrout, in *Handbook of Dynamical Systems* edited by B. Fiedler (Elsevier, Amsterdam, 2002), Vol. 2, pp. 3-54.
[11] N. Kopell and G. B. Ermentrout, Proc. Natl. Acad. Sci. U.S.A. **101**, 15 482 (2004).
[12] M. Bazhenov, N. Rulkov, J.-M. Fellous, and I. Timofeev, Phys. Rev. E **72**, 041903 (2005); M. I. Rabinovich, P. Varona, A. I. Selverston, and H. D. I. Abarbanel, Rev. Mod. Phys. **78**, 1213 (2006).
[13] G. S. Cymbalyuk, Q. Gaudry, M. A. Masino, and R. L. Calabrese, J. Neurosci. **22**, 10 580 (2002).
[14] R. J. Calin-Jageman, M. J. Tunstall, B. D. Mensh, P. S. Katz, and W. N. Frost, J. Neurophysiol. **98**, 2382 (2007).
[15] V. Matveev, A. Bose, and F. Nadim, J. Comput. Neurosci. **23**, 169 (2007).